Dynamical impurity in a tight-binding Hamiltonian model



2001 J. Phys. A: Math. Gen. 34 5795

(http://iopscience.iop.org/0305-4470/34/29/305)

INSTITUTE OF PHYSICS PUBLISHING JOURNAL OF PHYSICS A: MATHEMATICAL AND GENERAL

J. Phys. A: Math. Gen. **34** (2001) 5795–5814 PII: S0305-4470(01)20576-9

# Dynamical impurity in a tight-binding Hamiltonian model

**A Karina Chattah**[1] **and Manuel O Cáceres**[2,3]

[1] Centro Atómico Bariloche, Av. E. Bustillo Km 9.5, 8400 Bariloche, Argentina
[2] Centro Atómico Bariloche and Instituto Balseiro, CNEA and Universidad, Nacional de Cuyo, Av. E. Bustillo Km 9.5, 8400 Bariloche, Argentina

E-mail: chattah@famaf.unc.edu.ar and caceres@cab.cnea.gov.ar

Received 2 January 2001
Published 13 July 2001
Online at stacks.iop.org/JPhysA/34/5795

**Abstract**

We find the exact dynamics—in mean value—for a one-dimensional tight-binding model in the presence of a dynamical impurity (dichotomic process). Using the theorem of Bourret *et al* we prove that a 'dynamical localization' of the TB wave function electron is indeed generated by the stochastic impurity. Our results can also be interpreted in terms of a 'quasi-particle', representing the excitation of the system interacting with its surroundings. A lifetime and an energy can be associated with this quasi-particle. This lifetime appears as an irreversible process occurring due to the interaction with the stochastic impurity.

PACS numbers: 45.50.-j, 02.30.Hq, 05.10.Gg, 11.10.-m, 63.20.Kr, 71.38.-k

## 1. Introduction

Since the early days of the theory of dynamic disorder [1] it has been recognized that site-diagonal and off-diagonal *dynamical* disorder are relevant to study models of electron–phonon coupling in molecular solids; also, charge dynamics in columnar discotic liquid crystals leads to deal with dynamical disorder—i.e. disorder depending on the temperature—due to its intrinsic self-repair behaviour [2].

The question of the localization of the eigenstate in a static (quenched) disorder model has been extensively studied in the past [3]. At finite temperature the electrons are coupled to the thermal phonons and diffusion sets in; thus a natural way to study this phenomena is in the context of stochastic TB Hamiltonians. From the stochastic Hamiltonian approach it is possible to find an evolution equation for the average of the density matrix, in an analytical way [1, 4, 5], or from the numerical point of view [6]. It is also possible to set equations or

[3] Senior Independent Researcher associated with CONICET.

  

scaling analyses for the moments of the particle displacement [7]. Therefore non-anomalous versus anomalous quantum diffusion can be studied, depending on the model of the dynamical disorder. Nevertheless an exhaustive study of dynamical disorder does not seem to have drawn comparable attention, even when its analysis is also of great importance in transport physics in solids and polymers.

A better insight concerning the 'dynamical localization' (i.e. with a finite lifetime) could be achieved if we were able to characterize the localization phenomena of a particle in a *one dynamical impurity* model. For example, using this type of model one could simulate the stochastic transitions of a single *impurity* ion between different equivalent positions (i.e. a temperature-dependent trap in polymers [8]). A model of *one stochastic impurity* is also very interesting because it can be related to the problem of delocalization due to the measurement, i.e. the interaction with a detector apparatus [9].

In order to determine this program we need to model the *dynamical impurity* by means of some stochastic process which could ultimately (rigorously) be solved. Among the different types of dynamical impurities that can be treated analytically is the Gaussian delta-correlated one, but this Gaussian model cannot be put, in any limit, in correspondence with a static impurity. Then we would like to introduce an impurity noise that can be mapped with the static regime (i.e. zero temperature), as well as with the fast fluctuation regime (i.e. infinite temperature). Among the different processes that can fulfil these conditions is the dichotomous stochastic process originally introduced by Anderson [10] and Kubo [11]. Thus, instead of a delta-correlated noise, the use of an exponential decay correlation function, characterizing the dichotomic noise, represents a straightforward temperature-dependent generalization. This problem is technically more complicated than the white-noise case [12]. But, in particular, Bourret *et al* have proved many interesting theorems involving a functional of a dichotomous stochastic process, which will help us to find exact mean values [13, 14]. This kind of noise has also been introduced as dynamical disorder in the study of diffusion in a 1D classical chain [15], and in the analysis of the density matrix using semi-analytical methods [16]. Problems like these have also been considered in quantum diffusion models using a two-state Hamiltonian with dichotomic energies to explain electron transport in proteins [17, 18], for example.

In this paper we introduce a dynamical impurity of the site-disorder type in an ordered TB chain; a single off-diagonal dynamical impurity model can be solved in the same way. Consider the one-dimensional TB Hamiltonian of the form

$$H = H_0 + H_I(t) \tag{1}$$

where $H_0$ describes the one-band homogenous TB chain and the time-dependent impurity perturbation is characterized by

$$\boldsymbol{H}_I(t) = \varepsilon\, m(t)|l\rangle\langle l|. \tag{2}$$

Here $\varepsilon$ represents the amplitude of the dynamical impurity located at site $l$, the state $|l\rangle$ belongs to the Wannier basis and $m(t) \in \mathcal{R}_e$ is a dichotomous stochastic process[4] with a characteristic frequency rate $\nu/2$. Using this dichotomous noise, both of the regimes previously commented on will be covered: the static impurity is the $\nu \to 0$ case, while the fast fluctuation limit can be reached when $\nu \to \infty$.

Analysing the average time-dependent quantum amplitude $\langle G(t)\rangle$, i.e. the mean value (m.v.) of the Green function over the stochastic impurity, the dynamical localization phenomena can be studied. In addition the m.v. of the density of states (DOS) and the

[4] The corresponding master equation for $m(t)$ is $\dot{P} = \begin{pmatrix} -\nu/2 & \nu/2 \\ \nu/2 & -\nu/2 \end{pmatrix} P$. Then $\nu/2$ is the *frequency rate* for the dichotomic noise. In principle the temperature dependence $\nu = \nu(T)$ can be modelled in a general way: for our case we expect an increasing $\nu$ for increasing $T$.

inverse of the localization length $\lambda^{-1}$ can be calculated from our approach, so complementary information can be given from these quantities. These averaged DOS and $\lambda^{-1}$ lead us to associate an *effective* stationary system. We emphasize that the dynamics coming from $\langle G(t)\rangle$ cannot completely be reobtained from the analysis of the averaged DOS and $\lambda^{-1}$, because the Hamiltonian is stochastic. It is important to note that this problem will be solved analytically and the calculation of $\langle G\rangle$ will be an exact result.

The problem of a single static impurity ($\nu \to 0$) in a one-dimensional TB Hamiltonian has been solved for the diagonal and off-diagonal cases [19–21]. Consequently all the properties of the system can be given in terms of its Green function (i.e. DOS, localization length, wave function dynamics). Our aim in the stochastic impurity problem is to analyse the changes of all these properties in terms of the noise frequency $\nu$. This model helps us to understand the related problem of an arbitrary number of dynamical impurities, i.e. a fluctuating disordered medium.

The outline of this paper is as follows: in section 2.1 some general results concerning the Green function are described. In section 2.2 the method for obtaining the m.v. of the Green function in the presence of a dynamical impurity is discussed. In sections 3 and 4 one-particle properties in the dynamical impurity case are presented. Section 5 is concerned with a general discussion and results. The appendix is devoted to the Gaussian white-noise impurity case.

## 2. Green function with a dynamical impurity

In this section we study the properties of the m.v. TB Green function, when a dynamical impurity modifies stochastically the energy of a given site. First, we give general definitions and properties of the Green function.

### *2.1. General aspects of the Green function*

The Green function $G(z)$ associated with a Hamiltonian $H$ is defined as

$$(z - H)G(z) = I$$

where $z$ is a complex number with $\mathrm{Re}\,[z] = E$ representing the system energies and $\mathrm{Im}\,[z] = \eta$. The analytical structure of $G(z)$ is directly related to the spectrum of $H$: the poles are associated with the discrete energies and the branch cuts with the continuum spectrum. The DOS per site of the TB electron (or particle) is given in terms of the side limits of the Green function:

$$\pi \mathcal{D}_{\mathrm{DOS}}(E, n) = \mp \mathrm{Im}\, G^{\pm}_{n,n}(E) = \lim_{\eta \to 0^+} G_{n,n}(E \pm \mathrm{i}\eta). \tag{3}$$

If a localized state $\psi$ exists near the site $n_0$, its envelope decreases exponentially at large distances from its maximum; then the localization length $\lambda(E)$ is usually defined by Borland's criterion [20, 22]:

$$\lambda^{-1}(E) = -\lim_{|n-n_0|\to\infty} \frac{1}{|n - n_0|} \langle \ln |G_{n,n_0}| \rangle_{\mathrm{disorder}}.$$

Another criterion to understand the localization phenomena is the Anderson one, also used by Lloyd [23, 24]. Using Anderson's criterion we assume that the system is excited at a given site $n_0$ at time $t = 0$, so the quantum amplitude satisfies $A_n(t = 0) = \delta_{n,n_0}$. Then the solution of the time-dependent Schrödinger equation is related to the integration in the complex plane:

$$A_n(t) = \mathrm{i}G_{n,n_0}(t) = \mathrm{i} \int_{\mathrm{i}\eta-\infty}^{\mathrm{i}\eta+\infty} G_{n,n_0}(z) \exp(-\mathrm{i}zt) \frac{\mathrm{d}z}{2\pi} \qquad t > 0 \quad \eta > 0. \tag{4}$$

For a finite system this is an almost-periodic function, but for an infinite system the amplitude at $n_0$ will decay to zero unless there is a localized state near $n_0$. A localized state is therefore defined throughout this paper in terms of whether the diagonal element $iG_{n_0,n_0}(t)$ decays to zero or not.

We remark that, when studying a stochastic system, the useful quantity is the averaged Green function $\langle G\rangle_{\text{noise}}$. As a consequence all the physical quantities deduced from the m.v. $\langle G\rangle_{\text{noise}}$ will be averaged quantities over the stochastic realizations of the impurity. The temporal behaviour of $i\langle G_{n,n}(t)\rangle_{\text{noise}}$ comes in part from the poles of $\langle G(z)\rangle_{\text{noise}}$, so our point of view concerning the dynamical localization is analogous to the condition for the occurrence of *weak absence of diffusion*, as proved by Ishii with static disorder [25]. As a consequence of Ishii's conditions, when the imaginary part of the effective self-energies of the Green function is zero there is weak absence of diffusion. In our work the imaginary part of the effective self-energies is related to the imaginary part of the poles of $\langle G(z)\rangle_{\text{noise}}$. Then, when the poles have zero imaginary part there is a localized state in the weak sense; when this imaginary part is non-zero we define a dynamical localized state by virtue of its lifetime.

### 2.2. Dynamical impurity

In this section we analyse the averaged Green function for a single dynamical perturbation in a TB Hamiltonian. The method results in an exact expression for the m.v. of the Green function with a dynamical impurity; we start the calculation from the time-dependent Schrödinger equation. The model is described by the total Hamiltonian, equation (1), $H = H_0 + H_I(t)$ where the first term is the homogenous TB Hamiltonian written in the Wannier basis:

$$H_0 = \sum_n \varepsilon_0 |n\rangle\langle n| + \sum_n v_0 |n\rangle\langle n \pm 1| \tag{5}$$

where $\varepsilon_0$ is the electronic energy of an isolated orbital and $v_0 > 0$ is the hopping constant between nearest-neighbour sites. The perturbation is $H_I(t) = \varepsilon m(t) V_l$, where $V_l = |l\rangle\langle l|$ and we take $\varepsilon > 0$. Here $m(t) \in \mathcal{R}_e$ is a dichotomous stochastic process that jumps between two states represented by the values $\pm 1$ with frequency rate $\nu/2$, so its m.v. and the second moment are

$$\langle m(t)\rangle = m(0)\exp[-\nu t]$$
$$\langle m(t)m(s)\rangle = \exp[-\nu|t-s|].$$

The bracket denotes the average over the realizations of the stochastic process $m(t)$ see footnote 4. Note that it is important to consider the initial condition $m(0)$ in order to map, in the limit $\nu = 0$, with the static impurity case. To find the Green function of the system averaged over all realizations of the noise we follow the line of Bourret [13]. The wave equation of the system $i\hbar\dot{\psi} = (H_0 + H_I(t))\psi$ can be formally integrated as

$$\psi(t) = \exp[-itH_0/\hbar]\psi(0) - \frac{i\varepsilon}{\hbar}\int_0^t ds \exp[-i(t-s)H_0/\hbar]m(s)V_l\psi(s).$$

Note that, because the stochastic perturbation $H_I(t)$ is Hermitian, the wave function will be normalized for each realization of the dynamical impurity [26]. Inserting this expression in the right-hand side of the wave equation and taking the average over the stochastic process, we obtain

$$\langle\dot{\psi}(t)\rangle = -\frac{i}{\hbar}H_0\langle\psi(t)\rangle - \frac{i\varepsilon}{\hbar}\langle m(t)\rangle V_l \exp[-itH_0/\hbar]\psi(0) - \left(\frac{\varepsilon}{\hbar}\right)^2\int_0^t ds\, V_l \exp[-i(t-s)H_0/\hbar]V_l\langle m(t)m(s)\psi(s)\rangle. \tag{6}$$

To find a closed expression for the average $\langle\psi(t)\rangle$ it is necessary to factorize the moment $\langle m(t)m(s)\psi(s)\rangle$; this can be done using a special theorem valid for a dichotomous process [13]. This theorem says that, if $\Phi[m(t)]$ is a functional of the dichotomous process, involving earlier times than $s$, then for $t > s$ it follows that

$$\langle m(t)m(s)\Phi(s)\rangle = \langle m(t)m(s)\rangle\langle\Phi(s)\rangle.$$

We remark that this result is also valid when the mean value of the dichotomous process is not zero (as in our case). Replacing this last equation in (6) we finally obtain the averaged wave equation:

$$\langle\dot{\psi}(t)\rangle = -\frac{\mathrm{i}}{\hbar}H_0\langle\psi(t)\rangle - \frac{\mathrm{i}\varepsilon}{\hbar}m(0)V_l\exp[-t(\mathrm{i}/\hbar H_0+\nu)]\psi(0) - \left(\frac{\varepsilon}{\hbar}\right)^2\int_0^t \mathrm{d}s\, V_l\exp[-(t-s)(\mathrm{i}H_0/\hbar+\nu)]V_l\langle\psi(s)\rangle. \tag{7}$$

Now we take the Laplace transform of this equation using the definition $\langle\psi(z)\rangle = \int_0^\infty \mathrm{d}t\,\langle\psi(t)\rangle\exp[-zt]$ and we note that the Laplace transform and its inverse are denoted by their arguments $z$ and $t$. The averaged Green function is defined by $\langle G(z)\rangle\psi(0) = -\frac{\mathrm{i}}{\hbar}\langle\psi(-\frac{\mathrm{i}}{\hbar}z)\rangle$. Then from (7) we obtain

$$\langle G(z)\rangle = G_1(z)(I + \varepsilon m(0)V_l G_0(z+\mathrm{i}\hbar\nu)). \tag{8}$$

Here $I$ is the identity operator and $G_0 = (z-H_0)^{-1}$ is the homogenous Green function. The $G_0$ has matrix elements $\langle n|G_0|m\rangle = F\rho^{|n-m|}$, where $F = 1/(2v_0\sqrt{x^2-1})$, $\rho = x-\sqrt{x^2-1}$, with $x = (z-\varepsilon_0)/2v_0$. Here $\sqrt{x^2-1}$ denotes the square root of a complex number whose imaginary part has the same sign as $\mathrm{Im}\,[x]$ and the real part of $\sqrt{x^2-1}$ has the same sign as $\mathrm{Re}\,[x]$. The Green function $G_1(z)$ represents one impurity in the site $l$, with an effective additional energy depending on $z$ given by $\tilde{\varepsilon}_d(z) = \varepsilon^2[G_0(z+\mathrm{i}\hbar\nu)]_{l,l}$. Then

$$G_1(z) = [z - H_0 - \varepsilon^2 V_l G_0(z+\mathrm{i}\hbar\nu)V_l]^{-1} = [z - H_0 - \tilde{\varepsilon}_d(z)V_l]^{-1}.$$

In the last step we have used the property $V_l A V_l = A_{l,l}$ valid for any operator $A$. From (8) we find for the diagonal elements of $\langle G(z)\rangle$ the result

$$\langle G(z)_{l,l}\rangle = \frac{F^{-1}(z+\mathrm{i}\hbar\nu)+\varepsilon m(0)}{F^{-1}(z)F^{-1}(z+\mathrm{i}\hbar\nu)-\varepsilon^2} \tag{9}$$

and similarly for the off-diagonal elements

$$\langle G(z)_{n,l}\rangle = F(z)\rho(z)^{|n-l|}\frac{1+\varepsilon m(0)F(z+\mathrm{i}\hbar\nu)}{1-\varepsilon^2F(z)F(z+\mathrm{i}\hbar\nu)} = \rho(z)^{|n-l|}\langle G(z)_{l,l}\rangle. \tag{10}$$

This is one of the goals of this paper. From this exact result we can analyse the topological structure of the averaged Green function.

## 3. Averaged density of states for the TB electron

From now on, we take the band centre in $\varepsilon_0 = 0$ and give the energies in units of the half band width $2v_0$, so using dimensional parameters $x \to z/2v_0$, $\hbar\nu \to \hbar\nu/2v_0$ and $\varepsilon \to \varepsilon/2v_0$ (from now on we assume $2v_0 = 1$). Taking the initial condition of the dichotomous process $m(0) = 1$, the expression of the diagonal elements (9) with $\hbar = 1$ is

$$\langle G(x)_{l,l}\rangle = \frac{\sqrt{(x+\mathrm{i}\nu)^2-1}+\varepsilon}{\sqrt{x^2-1}\sqrt{(x+\mathrm{i}\nu)^2-1}-\varepsilon^2}. \tag{11}$$

The contribution to the averaged DOS of the particle, in the impurity site, is related to the imaginary part of the lateral averaged Green function for values of energy $x = E$ on the real axis:

$$\pi \mathcal{D}_{\mathrm{DOS}}(x,l) = -\mathrm{Im}\,\langle G^{+}(x)_{l,l}\rangle = -\lim_{\eta\to 0^{+}} \mathrm{Im}\left[\frac{\sqrt{(x+\mathrm{i}(\nu+\eta))^2-1}+\varepsilon}{\sqrt{(x+\mathrm{i}\eta)^2-1}\sqrt{(x+\mathrm{i}(\nu+\eta))^2-1}-\varepsilon^2}\right].$$

We have calculated this exact averaged DOS using the lateral Green function $\langle G^{+}\rangle$ because the imaginary quantity added to $x$ is always positive, $\nu > 0$. The expression for $\mathcal{D}_{\mathrm{DOS}}$ is calculated taking the square root of a complex number $z^{1/2} = \sqrt{(|z|+a)/2}+\mathrm{i}\,\mathrm{sgn}[b]\sqrt{(|z|-a)/2}$, where $z = a+\mathrm{i}b$, and also taking into account that $\sqrt{z^2-1} = \sqrt{z-1}\sqrt{z+1}$.

In figure 1 we show $\mathcal{D}_{\mathrm{DOS}}(x,l)$ with the energy given in units of the half band width for an impurity intensity $\varepsilon = \sqrt{3}$, and for several frequency values $\nu$. For the static impurity $\nu = 0$, we reobtain the continuum spectrum of $H_0$ (energy band of extended states) corresponding to the branch cut for $G_0$ defined by $|x| \leqslant 1$ with real $x$ and a delta peak located at $x_S = \sqrt{\varepsilon^2+1}$ (localized state), see figure 1($a$). For $\nu > 0$ we see that the stochastic nature of the substitutional site modifies the averaged DOS at this site $l$. Instead of having a delta function there is a maximum near the localized energy $x_S$ and also a continuum of states outside the band appears. When the frequency is large enough $\hbar\nu \gg 2v_0$ (in dimensional units) the continuum outside the band starts to disappear, and the right maximum of the $\mathcal{D}_{\mathrm{DOS}}$ (for $x \geqslant 0$) is very close to the band edge (giving a similar behaviour to resonant-like states, but outside the band). When the frequency $\nu$ is infinite the contribution to the averaged DOS is the one corresponding to the homogenous TB case. This happens because the rapid temporal fluctuations of the noise $m(t)$ erases the effect of a different energy in the impurity site.

For the averaged inverse localization length $\lambda^{-1}(x)$, calculated from the off-diagonal elements (10), we obtain the upper bound approximation with energy $x = E$:

$$\lambda^{-1}(x) = -\ln[\rho(x)] = \ln\left[x+\sqrt{x^2-1}\right].$$

Then $\mathrm{Re}\,[\lambda^{-1}(x)] = 0$ for $|x| < 1$, and for values $|x| > 1$ we obtain $\mathrm{Re}\,[\lambda^{-1}(x)] \neq 0$, see figure 1; this means that the states outside the band have a certain degree of localization while the states inside the band are of an extended nature, as in the static case. Note that the same expression is obtained for the static impurity case. This is the information given by $\mathcal{D}_{\mathrm{DOS}}$ and the inverse localization length $\lambda^{-1}$.

In order to analyse how the dynamical impurity affects the wave function of the TB electron it is necessary to characterize the behaviour of the time-dependent function $\langle G_{l,l}(t)\rangle$.

## 4. Dynamics of the TB electron

In this section we find the temporal behaviour of the mean value amplitude $A_l(t) = \mathrm{i}\langle G_{l,l}(t)\rangle$ in order to describe the averaged dynamics of the TB electron as a function of the frequency $\nu$, so we can get an insight into the characteristics of the 'dynamical localization' phenomena. Assuming that, at $t = 0$ the particle is in the impurity site, we calculate for $t > 0$

$$\langle G_{l,l}(t)\rangle = \int_{\mathrm{i}\eta-\infty}^{\mathrm{i}\eta+\infty} \langle G_{l,l}(x)\rangle \exp(-\mathrm{i}xt)\frac{\mathrm{d}x}{2\pi}. \tag{12}$$

Note that, because $\eta > 0$, the last expression corresponds to the use of $\langle G^{+}\rangle$ which is appropriate for $t > 0$, see equation (3). To perform this integration in the complex plane, it is necessary to know the regions of non-analyticity of $\langle G_{l,l}(x)\rangle$. In most cases the integral (12) cannot be evaluated explicitly, so knowledge of the singularities of the Green function may give information about the asymptotic behaviour of $\langle G_{l,l}(t)\rangle$ at long time [27].

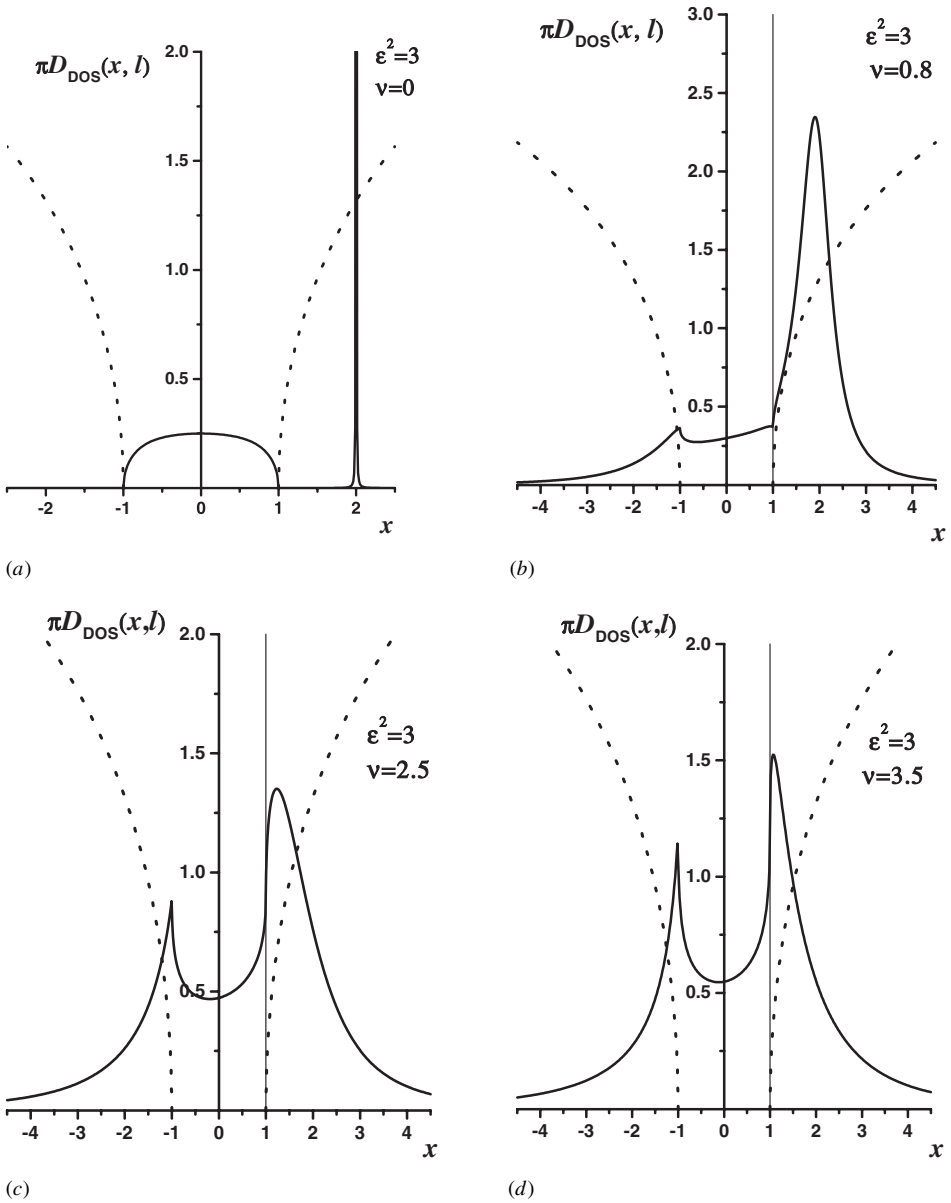


**Figure 1.** Averaged DOS at the impurity site $\pi\mathcal{D}_{\mathrm{DOS}}(x, l)$ versus energy $x$ for $\varepsilon^2 = 3$ and different values of frequency $\nu$. The dotted curves corresponds to the inverse localization length $\lambda^{-1}(x)$. The vertical line denotes the band edge at $x = 1$. For $\nu = 0$ we reobtain the static impurity case, and when $\nu \gg 1$ the system approaches, on average, the homogenous TB model. Note that for $\nu \gtrsim \varepsilon^2$ the peak in the averaged DOS is very near the band edge (from outside).

### *4.1. Singularities of* $\langle G_{l,l}(x)\rangle$

From expression (11) we can see that the diagonal element of the averaged Green function is defined through square roots for two complex numbers. Then there are two branch cuts that must not be crossed in order to define an analytical continuation of these functions, keeping

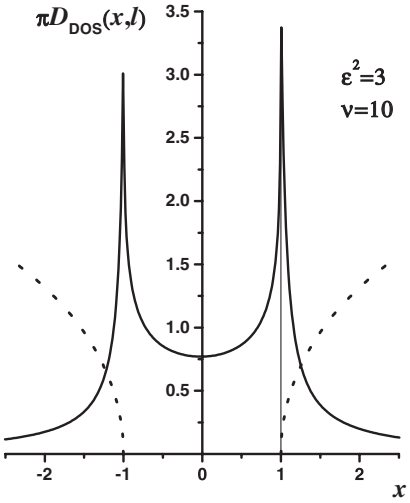


(*e*) **Figure 1.** (Continued.)

$\langle G_{l,l}(x)\rangle$ univalued. One of these branch cuts coincides with the continuum spectrum of $G_0$, defined by $\mathrm{Im}\,[x] = 0$ and $|x| \leqslant 1$; the other region of non-analyticity appears because of the 'dynamical nature' of the impurity and it is given by $\mathrm{Im}\,[x] = -\nu$ and $|\mathrm{Re}\,[x]| \leqslant 1$ (so we call this cut the *dynamical branch cut*).

The discrete singularities of the function $\langle G_{l,l}(x)\rangle$ are the zeros of the denominator:

$$F^{-1}(x)F^{-1}(x + \mathrm{i}\nu) - \varepsilon^2 = 0. \tag{13}$$

It is possible to modify this equation to a quartic one and solve this by introducing the change of variable $x = u - \mathrm{i}\nu/2$. Therefore we obtain

$$((u - \mathrm{i}\nu/2)^2 - 1)((u + \mathrm{i}\nu/2)^2 - 1) - \varepsilon^4 = 0. \tag{14}$$

The zeros of this quartic equation in the original variable $x_k(\nu, \varepsilon) = u_k(\nu, \varepsilon) - \mathrm{i}\nu/2$ can be written in terms of the parameters $(\nu, \varepsilon)$ in the form

$$\begin{aligned} x_k(\nu, \varepsilon) &= \pm\sqrt{1 - \frac{\nu^2}{4} + \sqrt{\varepsilon^4 - \nu^2}} - \mathrm{i}\frac{\nu}{2} \qquad k = 1, 2 \\ x_k(\nu, \varepsilon) &= \pm\sqrt{1 - \frac{\nu^2}{4} - \sqrt{\varepsilon^4 - \nu^2}} - \mathrm{i}\frac{\nu}{2} \qquad k = 3, 4. \end{aligned} \tag{15}$$

Before going into further details we have to understand when these solutions produce poles in $\langle G_{l,l}(x)\rangle$. This question is not trivial because of the presence of square roots in $F(x)$ and $F(x + \mathrm{i}\nu)$ (see (11)). We adopt the usual convention:

$$\begin{aligned} &\mathrm{sgn}\left[\mathrm{Re}\left[\sqrt{x^2 - 1}\right]\right] = \mathrm{sgn}[\mathrm{Re}\,[x]] \\ &\mathrm{sgn}\left[\mathrm{Im}\left[\sqrt{x^2 - 1}\right]\right] = \mathrm{sgn}[\mathrm{Im}\,[x]] \\ &\mathrm{sgn}\left[\mathrm{Re}\left[\sqrt{(x + \mathrm{i}\nu)^2 - 1}\right]\right] = \mathrm{sgn}[\mathrm{Re}\,[x]] \\ &\mathrm{sgn}\left[\mathrm{Im}\left[\sqrt{(x + \mathrm{i}\nu)^2 - 1}\right]\right] = \mathrm{sgn}[\mathrm{Im}\,[x] + \nu]] \end{aligned}$$

where $\mathrm{sgn}[f]$ means to take the sign of the quantity $f$. Inserting these conditions in (13), we find a clear criterion that must fulfil the imaginary parts of the roots $x_k(\nu, \varepsilon)$ in order to be *true*

poles of the averaged Green function $\langle G_{l,l}(x)\rangle$. So

$$\mathrm{sgn}[\mathrm{Im}\,[x_k]]\mathrm{sgn}[\mathrm{Im}\,[x_k]+\nu]=-1 \tag{16}$$

unless $\mathrm{Re}\,[\sqrt{x^2-1}]\mathrm{Im}\,[\sqrt{(x+\mathrm{i}\nu)^2-1}] = \mathrm{Im}\,[\sqrt{x^2-1}]\mathrm{Re}\,[\sqrt{(x+\mathrm{i}\nu)^2-1}] = 0$. Note that the case $\nu = 0$ must be considered with special care. With condition (16) we can now investigate the validity of (15) in the space of the parameters $(\nu, \varepsilon)$.

First, analysing the roots $x_1, x_2$ we see that they satisfy (16) for all $\nu > 0$. In addition they have $\mathrm{Im}\,[x_k] < 0$ for $k = 1, 2$.

Second, analysing $x_3, x_4$ we see that the only region in the space $(\nu, \varepsilon)$ where (16) is not satisfied is characterized by the values $\varepsilon > 1$ and $0 < \nu \leqslant \sqrt{\varepsilon^4-1}$; but precisely for this region in $(\nu, \varepsilon)$ we found that $\mathrm{Im}\,[x_3] \geqslant 0$, which would give the wrong behaviour (divergent) for long times. For $\varepsilon < 1$, these roots satisfy (16) for all $\nu > 0$.

Now we check the special case $\nu = 0$ corresponding to the static impurity. In this case there is only one pole: $x_1(0, \varepsilon) = x_S$ or $x_2(0, \varepsilon)$, depending on whether $m(0) = \pm 1$. In this case $\mathrm{Im}\,[x_k(0, \varepsilon)] = 0$ so, as usual, we add a small parameter $\eta \to 0$ in order to calculate the complex square roots. For $\varepsilon < 1$, we find that (16) is not fulfilled by the roots $x_{3,4}(0, \varepsilon)$, and for $\varepsilon > 1$ they are not poles when $\nu = 0$. On the other hand, $x_{1,2}(0, \varepsilon)$ give $\mathrm{Im}\,[\sqrt{x^2-1}] \to 0$ (for all $\varepsilon$) so we do not need to fulfil (16). Therefore we have to choose between $x_1$ and $x_2$. This selection comes from the fact that, when $\nu = 0$, $x_2$ for $m(0) = 1$ (or $x_1$ for $m(0) = -1$) is also a root of $\sqrt{(x+\mathrm{i}\nu)^2-1}+\varepsilon$ (the numerator of $\langle G_{l,l}(x)\rangle$). Then some terms are simplified and we finally arrive at the expected pole when $\nu = 0$.

This complete analysis tells that the poles of $\langle G_{l,l}(x)\rangle$ are (assuming the initial condition $m(0) = 1$ as in (11))

$$\begin{aligned}
&x_1 && \text{for} \quad \varepsilon > 0 \quad \nu \geqslant 0\\
&x_2 && \text{for} \quad \varepsilon > 0 \quad \nu > 0\\
&x_3, x_4 && \text{for} \quad 0 < \varepsilon \leqslant 1 \quad \nu > 0\\
&x_3, x_4 && \text{for} \quad \varepsilon > 1 \quad \nu > \sqrt{\varepsilon^4-1}.
\end{aligned} \tag{17}$$

Having these facts in mind we now give a fine expression for the poles, in order to write down more explicitly the real and imaginary parts of $x_k(\nu, \varepsilon)$.

First we study $k = 1, 2$. We define the complex functions

$$c_I(\nu, \varepsilon) = \sqrt{1-\frac{\nu^2}{4}+\mathrm{i}\sqrt{\nu^2-\varepsilon^4}} \qquad \text{for} \quad \nu > \varepsilon^2$$

and

$$f_I(\nu, \varepsilon) = 1-\frac{\nu^2}{4}+\sqrt{\varepsilon^4-\nu^2} \qquad \text{for} \quad \nu \leqslant \varepsilon^2.$$

Then for $\nu > \varepsilon^2$ we get $x_k(\nu, \varepsilon) = \pm\mathrm{Re}\,[c_I(\nu, \varepsilon)] + \mathrm{i}(\pm\mathrm{Im}\,[c_I(\nu, \varepsilon)] - \frac{\nu}{2})$, and it is possible to see that in this case they always have non-vanishing real and imaginary parts. For $\nu \leqslant \varepsilon^2$ the pole $x_k$ can be purely imaginary, if $f_I(\nu, \varepsilon) < 0$, or not if $f_I(\nu, \varepsilon) > 0$. Then, separating different regions in the space $(\nu, \varepsilon)$ and writing explicitly the real and imaginary parts of $x_k(\nu, \varepsilon)$, for $\varepsilon^2 < 2$ we obtain

$$x_k(\nu, \varepsilon) = \pm\sqrt{f_I(\nu, \varepsilon)} - \mathrm{i}\frac{\nu}{2} \qquad \text{for} \quad \nu \leqslant \varepsilon^2 \tag{18}$$

and for $\varepsilon^2 \geqslant 2$

$$\begin{aligned}
x_k(\nu, \varepsilon) &= \mathrm{i}\left(\pm\sqrt{|f_I(\nu, \varepsilon)|}-\frac{\nu}{2}\right) && \text{for} \quad 2\sqrt{\varepsilon^2-1} < \nu \leqslant \varepsilon^2\\
x_k(\nu, \varepsilon) &= \pm\sqrt{f_I(\nu, \varepsilon)} - \mathrm{i}\frac{\nu}{2} && \text{for} \quad 0 < \nu \leqslant 2\sqrt{\varepsilon^2-1}.
\end{aligned} \tag{19}$$

Now for $k = 3, 4$ we define $c_{II}(\nu, \varepsilon) = \sqrt{1 - \frac{\nu^2}{4} - \mathrm{i}\sqrt{\nu^2 - \varepsilon^4}}$ with $\nu > \varepsilon^2$, and $f_{II}(\nu, \varepsilon) = 1 - \frac{\nu^2}{4} - \sqrt{\varepsilon^4 - \nu^2}$ with $\nu \leqslant \varepsilon^2$. Doing the same kind of analysis as before, we have for $\nu > \varepsilon^2$, $x_k(\nu, \varepsilon) = \pm\mathrm{Re}\,[c_{II}(\nu, \varepsilon)] + \mathrm{i}(\pm\mathrm{Im}\,[c_{II}(\nu, \varepsilon)] - \frac{\nu}{2})$. For $\nu \leqslant \varepsilon^2$ we separate three regions, depending on the value of $\varepsilon$. For $\varepsilon \leqslant 1$:

$$x_k(\nu, \varepsilon) = \pm\sqrt{f_{II}(\nu, \varepsilon)} - \mathrm{i}\frac{\nu}{2} \qquad \text{for} \quad \nu \leqslant \varepsilon^2 \tag{20}$$

for $1 < \varepsilon^2 < 2$:

$$\begin{aligned} x_k(\nu, \varepsilon) &= \pm\sqrt{f_{II}(\nu, \varepsilon)} - \mathrm{i}\frac{\nu}{2} \qquad && \text{for} \quad 2\sqrt{\varepsilon^2 - 1} < \nu \leqslant \varepsilon^2 \\ x_k(\nu, \varepsilon) &= \mathrm{i}\left(\pm\sqrt{|f_{II}(\nu, \varepsilon)|} - \frac{\nu}{2}\right) \qquad && \text{for} \quad \sqrt{\varepsilon^4 - 1} < \nu \leqslant 2\sqrt{\varepsilon^2 - 1} \end{aligned} \tag{21}$$

and for $\varepsilon^2 \geqslant 2$:

$$x_k(\nu, \varepsilon) = \mathrm{i}\left(\pm\sqrt{|f_{II}(\nu, \varepsilon)|} - \frac{\nu}{2}\right) \qquad \text{for} \quad \sqrt{\varepsilon^4 - 1} < \nu \leqslant \varepsilon^2. \tag{22}$$

We remark—once again—that in all the region $(\nu, \varepsilon)$ of validity the poles satisfy $\mathrm{Im}\,[x_k] < 0$ for all $k = 1, \ldots, 4$.

The information given by $\mathrm{Re}\,[x_k]$ and $\mathrm{Im}\,[x_k]$ is now related to the *energy* and the inverse of the *lifetime* of an excitation or 'quasi-particle', defined from the TB electron in interaction with the surroundings (the fluctuating impurity) [28].

In figure 2 we see the plots of $\mathrm{Re}\,[x_k]$ versus $\mathrm{Im}\,[x_k]$ in the complex plane for fixed values of $\varepsilon < 1$ and $\varepsilon > 1$, parametrized by the frequency $\nu$, changing continuously from $\nu = 0$ to $\infty$. In figures 3(*a*) and (*b*), we show in the space $(\nu, \varepsilon)$ the different regions for the behaviour of $x_k$, indicating the sign of $f_\alpha(\nu, \varepsilon)$ (or the presence of $c_\alpha(\nu, \varepsilon)$ if it corresponds) separately for the cases $k = 1, 2$ and 3, 4.

In the large frequency limit we can expand $x_{1,2}(\nu, \varepsilon) = \pm c_I(\nu, \varepsilon) - \mathrm{i}\frac{\nu}{2}$ and $x_{3,4}(\nu, \varepsilon) = \pm c_{II}(\nu, \varepsilon) - \mathrm{i}\frac{\nu}{2}$, obtaining

$$\begin{aligned} x_1 &= 1 - \frac{\varepsilon^4}{2\nu^2} - \mathrm{i}\frac{\varepsilon^4}{\nu^3} + \mathcal{O}\left(\frac{\varepsilon^8}{4\nu^4} + \mathrm{i}\frac{4\varepsilon^4}{\nu^6}\right) \\ x_4 &= -\left(1 - \frac{\varepsilon^4}{2\nu^2}\right) - \mathrm{i}\frac{\varepsilon^4}{\nu^3} + \mathcal{O}\left(\frac{\varepsilon^8}{4\nu^4} + \mathrm{i}\frac{4\varepsilon^4}{\nu^6}\right) \\ x_3 &= 1 - \frac{\varepsilon^4}{2\nu^2} - \mathrm{i}\nu + \mathcal{O}\left(\frac{\varepsilon^8}{4\nu^4} + \mathrm{i}\frac{4\varepsilon^4}{\nu^6}\right) \\ x_2 &= -\left(1 - \frac{\varepsilon^4}{2\nu^2}\right) - \mathrm{i}\nu + \mathcal{O}\left(\frac{\varepsilon^8}{4\nu^4} + \mathrm{i}\frac{4\varepsilon^4}{\nu^6}\right). \end{aligned} \tag{23}$$

These expressions show that the value of the parameter $\varepsilon$ takes part in the large frequency limit $\nu$. When $\nu \gg \varepsilon^2$ the poles $x_1, x_4$ approach the branch cut on the real axis and especially to the end branch points $\pm 1$, while the poles $x_3, x_2$ go to the 'dynamical branch cut' (this branch goes to $-\mathrm{i}\infty$ in the large frequency limit $\nu$).

It is known that the dichotomous process covers the Gaussian white-noise case in the limit $\varepsilon^2 \to \infty, \nu \to \infty$ with $\varepsilon^2/\nu \to D/2$, where $D$ is the intensity of the Gaussian process [12]. In this case, we investigate the poles separating two different cases, depending on the magnitude of $D$.

In the case $D < 2$ we get $\varepsilon^2 < \nu$. Then the poles in this limit are

$$\begin{aligned} x_1 &= \sqrt{1 - \frac{D^2}{4}} \qquad & x_4 &= -\sqrt{1 - \frac{D^2}{4}} \\ x_3 &= \sqrt{1 - \frac{D^2}{4}} - \mathrm{i}\infty \qquad & x_2 &= -\sqrt{1 - \frac{D^2}{4}} - \mathrm{i}\infty \end{aligned} \tag{24}$$

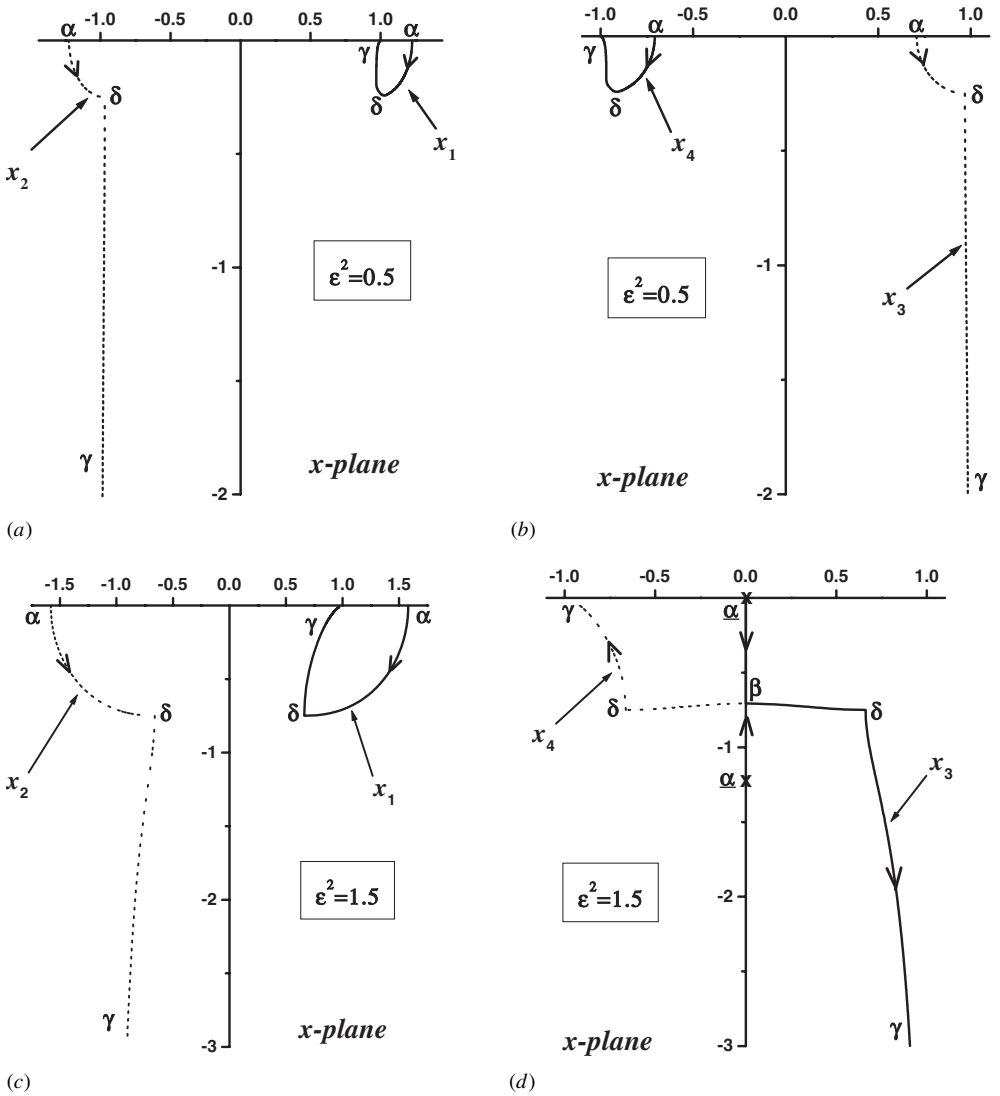


**Figure 2.** Position of the poles of $\langle G_{l,l}(x)\rangle$ in the complex $x$ *plane* parametrized with the frequency $\nu \in [0, \infty)$ for $\varepsilon^2 = 0.5$, 1.5 and 3. The arrows indicate the direction of increasing frequency $\nu$. In (*a*), (*c*), (*e*) we show the poles $x_1$, $x_2$; in (*b*), (*d*), (*f*) we show the poles $x_3$, $x_4$. The set of points $\alpha$, $\underline{\alpha}$, $\beta$, $\delta$, $\gamma$ are to be especially noted: the $\alpha$ points correspond to $\nu = 0$, $\underline{\alpha} \to \nu = \sqrt{\varepsilon^4 - 1}$, $\beta \to \nu = 2\sqrt{\varepsilon^2 - 1}$, $\delta \to \nu = \varepsilon^2$, $\gamma \to \nu \ll 1$.

and these poles are inside the branch cuts. The structure of (24) is similar to (23). Nevertheless we expect a different dynamical $\langle G_{l,l}(t)\rangle$ from both results, because the low correlation limit $\nu^{-1} \gg 1$, for a dichotomous process, is different from a Gaussian white-noise process.

In the case $D > 2$ we get $\varepsilon^2 > \nu$. Then in the Gaussian white-noise limit the poles $x_{1,2}$ are

$$x_1 = -\mathrm{i}\sqrt{\frac{D^2}{4} - 1} \qquad x_2 = \mathrm{i}\sqrt{\frac{D^2}{4} - 1} - \mathrm{i}\infty \tag{25}$$

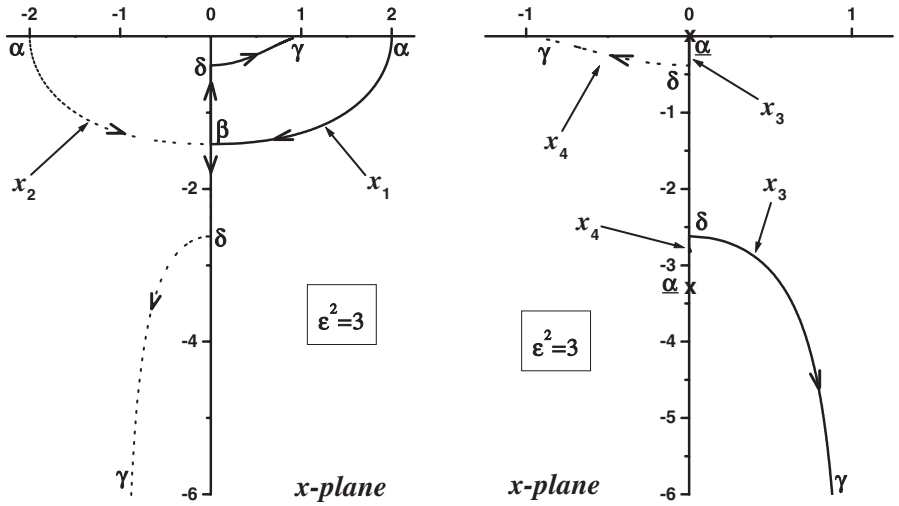


(*e*) (*f*)

**Figure 2.** (Continued.)

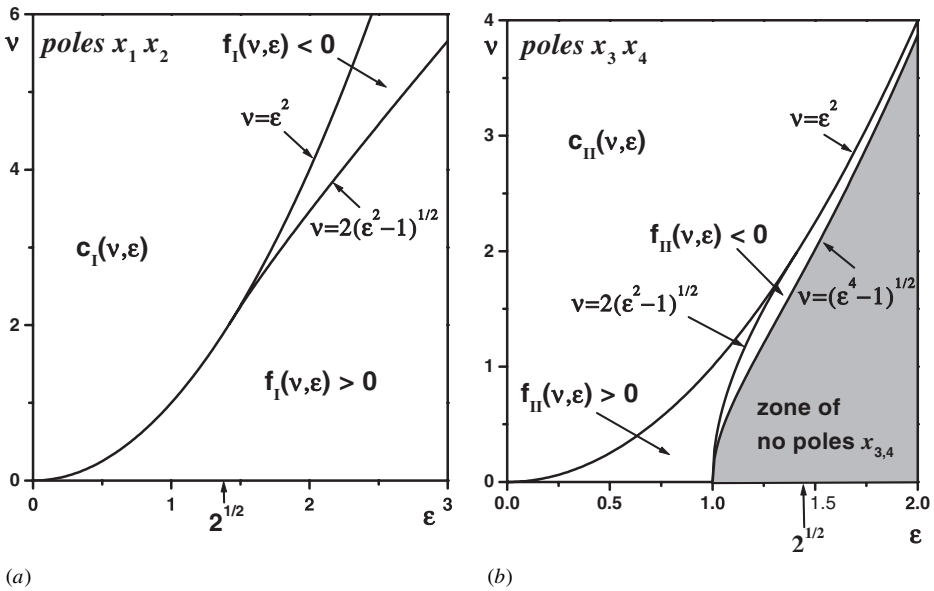


(*a*) (*b*)

**Figure 3.** Structure of the poles of $\langle G_{l,l}(x)\rangle$ in the parameter space $(\nu, \varepsilon)$. The functions $f(\nu, \varepsilon)$ and $c(\nu, \varepsilon)$ are given in the text. When $f(\nu, \varepsilon) < 0$ the poles are purely imaginary. In (*a*) poles $x_1$, $x_2$, these poles are allowed in all the space; (*b*) poles $x_3$, $x_4$; in this figure we have marked the zone of no poles $x_{3,4}$.

so $x_1$ is under the branch cut on the real axis and $x_2$ is over the 'dynamical branch cut'. In this case the other roots $x_{3,4}$ are not poles of the Green function, because the condition $\nu^2 > \sqrt{\varepsilon^4 - 1}$ (for $\varepsilon > 1$) would imply $D < 2$. To test these results a direct alternative analysis for the Gaussian white-noise case is covered in the appendix.

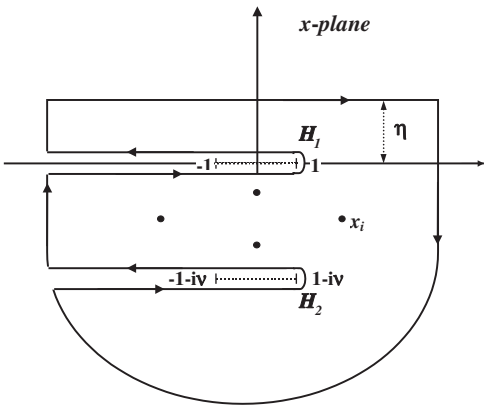


**Figure 4.** Contour of integration $\mathcal{C}$ in the *x plane* for obtaining $\langle G_{l,l}(t)\rangle$. The paths $\mathcal{H}_1$ and $\mathcal{H}_2$ correspond to the integral around the branch cuts in $\mathrm{Im}\,[x] = 0$ and $-\nu$, respectively. The dots $x_i$ corresponds to the poles always situated between the branch cuts.

### *4.2. Evaluating* $\langle G_{l,l}(t)\rangle$

Taking into account the results of the previous section we now perform the integral (12) in the complex plane following a closed path $\mathcal{C}$. This contour closes the line $[\mathrm{i}\eta - \infty, \mathrm{i}\eta + \infty]$ with a semicircle in the lower complex semi-plane, rounding the branch cuts as shown in figure 4. The path encloses all the poles of $\langle G_{l,l}(x)\rangle$, because they are in the interior of $\mathcal{C}$ having $\mathrm{Im}\,[x_k] \leqslant 0$ for all $k$. Therefore the theorem of residues, $\oint_{\mathcal{C}}\langle G_{l,l}(x)\rangle \exp[-\mathrm{i}xt]\,\mathrm{d}x = 2\pi\mathrm{i}\sum \mathrm{Res}[\langle G_{l,l}(x)\rangle \exp[-\mathrm{i}xt]]$, allows us to evaluate the integral (12), giving

$$\langle G_{l,l}(t)\rangle = \mathrm{i}\sum_k \operatorname*{Res}_{x=x_k}[\langle G_{l,l}(x)\rangle \exp[-\mathrm{i}xt]] - \int_{\mathcal{H}_1}\langle G_{l,l}(x)\rangle \exp[-\mathrm{i}xt]\,\frac{\mathrm{d}x}{2\pi} - \int_{\mathcal{H}_2}\langle G_{l,l}(x)\rangle \exp[-\mathrm{i}xt]\frac{\mathrm{d}x}{2\pi}. \tag{26}$$

The integrals over the paths $\mathcal{H}_i$ with $i = 1, 2$ are the integral around the branch cuts, on the real axis and on $-\mathrm{i}\nu$, respectively, see figure 4. It is possible to see that the integrals over the rest of the contour $\mathcal{C}$ vanish. Now, we calculate each of these terms separately.

*4.2.1. Contribution from the residues.* The first term of (26) involves the evaluation of the residues on the poles $x_k(\nu, \varepsilon)$ for $k = 1, 2, 3, 4$. First note that $x_k$ are *simple* poles, except for two cases $\nu = \varepsilon^2$ ($x_1 = x_3$ and $x_2 = x_4$) and for $\varepsilon > 1$ the frequency line $\nu = 2\sqrt{\varepsilon^2 - 1}$ ($x_3 = x_4$ if $1 < \varepsilon^2 < 2$ and $x_1 = x_2$ when $\varepsilon^2 > 2$). Then for the frequencies $\nu$ when $x_k$ are *simple* poles we obtain

$$\operatorname*{Res}_{x=x_k(\nu,\varepsilon)}[\langle G_{l,l}(x)\rangle \exp[-\mathrm{i}xt]] = M_1[x_k(\nu,\varepsilon)]\exp[-\mathrm{i}\mathrm{Re}\,[x_k]t]\exp[-|\mathrm{Im}\,[x_k]|t] \tag{27}$$

where

$$M_1[x_k(\nu,\varepsilon)] = \frac{\varepsilon^2}{2\,u_k(\nu,\varepsilon)}\frac{\sqrt{(u_k(\nu,\varepsilon)+\mathrm{i}\nu/2)^2 - 1} + \varepsilon}{(u_k^2(\nu,\varepsilon) + \frac{\nu^2}{4} - 1)}. \tag{28}$$

Here we have used the definition of $u_k(\nu,\varepsilon) = x_k(\nu,\varepsilon)+\mathrm{i}\nu/2$ given before (14). The result (27) is valid for all times $t$. From this expression it is possible to see that, in the limit of large values of $\nu$, these functions are of the order

$$|M_1[x_{1,4}(\nu \gg 1, \varepsilon)]| \sim \frac{\varepsilon^2}{\nu} \qquad |M_1[x_{2,3}(\nu \gg 1, \varepsilon)]| \sim \frac{\varepsilon^3}{\nu^2}. \tag{29}$$

Then in the limit $\nu \gg 1$ the residues on the poles $x_{2,3}$ (approaching the 'dynamical branch cut') decrease faster than the residues from the poles $x_{1,4}$ that go to the band on the real axis (see figure 2).

For the particular frequency lines mentioned above $\nu = \varepsilon^2$ and $\nu = 2\sqrt{\varepsilon^2 - 1}$, $x_k$ are second order poles. Then the expression from the residues gives a temporal dependence of the form $\sim t \exp[-\mathrm{i}x_k t]$. This behaviour is slower than from *simple* poles, but even though this could be important we will not analyse these particular cases further in the present paper.

*4.2.2. Integral over the cuts $\mathcal{H}_i$.* To give a closed expression for (26), at least asymptotically, we have to perform the integrals over the branch cuts $\mathcal{H}_i$. First we ought to note that the integral around $\mathcal{H}_2$ gives

$$\int_{\mathcal{H}_2} \langle G_{l,l}(x)\rangle \exp[-\mathrm{i}xt]\,\frac{\mathrm{d}x}{2\pi} = \exp[-\nu t]\int_{\mathcal{H}_1} \langle G_{l,l}(x)\rangle \exp[-\mathrm{i}xt]\frac{\mathrm{d}x}{2\pi}.$$

Then we need only to know the integral over the cut $\mathcal{H}_1$. This integral can be written down in the following form:

$$\int_{\mathcal{H}_1} \langle G_{l,l}(x)\rangle \exp[-\mathrm{i}xt]\frac{\mathrm{d}x}{2\pi} = \int_0^2 \exp[-\mathrm{i}(1-r)t] \times \left\{ \frac{\varepsilon + t_+(r,\nu)}{\varepsilon^2 - \mathrm{i}\sqrt{r(2-r)}t_+(r,\nu)} - \frac{\varepsilon + t_-(r,\nu)}{\varepsilon^2 + \mathrm{i}\sqrt{r(2-r)}t_-(r,\nu)} \right\} \frac{\mathrm{d}r}{2\pi} \tag{30}$$

where $t_\pm(r,\nu) = \sqrt{(2 + r\exp[\pm\mathrm{i}\pi] + \mathrm{i}\nu)}\sqrt{(r\exp[\pm\mathrm{i}\pi] + \mathrm{i}\nu)}$. It is very difficult to find an exact expression for this integral, so we only expect to give the behaviour for $t \to \infty$. In the case when $\nu = 0$, $t_+(r,0) = -t_-(r,0)$ and the solution can be calculated as an infinite series for $\varepsilon > 1$, giving a contribution of the order of $\mathcal{O}(\varepsilon^{-2}t^{-3/2})$ to (30) [24]. Now we want to find the asymptotic behaviour for (30) when the 'dynamical impurity' is turned on, i.e. $\nu \neq 0$. Then we can see that $t_+(r,\nu) = t_-(r,\nu) = t(r,\nu)$ when $\nu$ is strictly non-zero, so the last integral becomes

$$\int_{\mathcal{H}_1} \langle G_{l,l}(x)\rangle \exp[-\mathrm{i}xt]\frac{\mathrm{d}x}{2\pi} = \int_0^2 \exp[-\mathrm{i}(1-r)t]\, g(r,\nu)\, \tilde{g}(r)\frac{\mathrm{d}r}{2\pi} \tag{31}$$

where

$$g(r,\nu) = 2\mathrm{i}\frac{(\varepsilon + t(r,\nu))t(r,\nu)}{\varepsilon^4 + r(2-r)(2-r+\mathrm{i}\nu)(-r+\mathrm{i}\nu)} \qquad \tilde{g}(r) = \sqrt{r(2-r)}. \tag{32}$$

We can integrate (31) by parts, taking into account that $\tilde{g}(0) = \tilde{g}(2) = 0$. Thus we obtain

$$\int_0^2 \exp[-\mathrm{i}(1-r)t]g(r,\nu)\,\tilde{g}(r)\frac{\mathrm{d}r}{2\pi} = \frac{1}{(-\mathrm{i}t)}\int_0^2 \exp[-\mathrm{i}(1-r)t] \times \left( g(r,\nu)\,\frac{(1-r)}{\sqrt{r(2-r)}} + g'(r,\nu)\,\tilde{g}(r) \right)\frac{\mathrm{d}r}{2\pi} \tag{33}$$

where $g'(r,\nu)$ means the first derivative with respect to $r$. Now we work out each term separately.

The first integral can be done taking into account that, when the time goes to infinity, the integrand oscillates very rapidly and the most important contribution to the integral comes from values near $r = 0$ and 2. Then, if $g(r,\nu)$ is a smooth function in the interval [0, 2], the approximation when $t \to \infty$ is given by

$$\int_0^2 \exp[-\mathrm{i}(1-r)t]\, g(r,\nu)\frac{(1-r)}{\sqrt{r(2-r)}}\frac{\mathrm{d}r}{2\pi} \sim \sqrt{\frac{e}{4\pi t}}\left[ g(0,\nu)\exp\left[-\mathrm{i}\left(t - \frac{\pi}{4}\right)\right] - g(2,\nu)\,\exp\left[\mathrm{i}\left(t - \frac{\pi}{4}\right)\right]\right] \tag{34}$$

where we have worked out the asymptotic behaviour of the integrals near the dominant points: $\int_0^\delta \mathrm{d}r\ \exp[-\mathrm{i}(1-r)t]/\sqrt{r(2-r)}$ and $\int_{2-\delta}^2 \mathrm{d}r\ \exp[-\mathrm{i}(1-r)t]/\sqrt{r(2-r)}$, by the stationary phase method [27].

The second term in (33) is of the same form as the integrand of (31), so once again we can integrate by parts. In general, if $g^n(r,\nu)$ denotes the derivative of the order $n$ with respect to $r$, we obtain

$$\int_0^2 \exp[-\mathrm{i}(1-r)t]\, g^n(r,\nu)\, \tilde{g}(r)\frac{\mathrm{d}r}{2\pi} = \frac{1}{(-\mathrm{i}t)}\int_0^2 \exp[-\mathrm{i}(1-r)t]\left(g^n(r,\nu)\tilde{g}'(r) + g^{n+1}(r,\nu)\tilde{g}(r)\right)\frac{\mathrm{d}r}{2\pi}.$$

Using this result and assuming that $g^n(r,\nu)$ are smooth functions in $[0,2]$, a similar approximation to that in (34) can be obtained for the first term; then, following the same arguments as before we finally arrive at an expansion

$$\int_{\mathcal{H}_1}\langle G_{l,l}(x)\rangle \exp[-\mathrm{i}xt]\frac{\mathrm{d}x}{2\pi} \sim \int_0^2 \exp[-\mathrm{i}(1-r)t]\tilde{g}'(r)\left(\frac{g(r,\nu)}{(-\mathrm{i}t)} + \frac{g'(r,\nu)}{(-\mathrm{i}t)^2} + \cdots\right)\frac{\mathrm{d}r}{2\pi}.$$

Therefore the dominant term, for $t\to\infty$, from the integral over the cut $\mathcal{H}_1$ comes from (34), so

$$\int_{\mathcal{H}_1}\langle G_{l,l}(x)\rangle \exp[-\mathrm{i}xt]\frac{\mathrm{d}x}{2\pi} \sim \sqrt{\frac{e}{\pi}}\frac{\nu}{2\varepsilon^4 t^{3/2}}\left[\exp\left[\mathrm{i}\left(t+\frac{\pi}{4}\right)\right]\left(\varepsilon\sqrt{1+\frac{2\mathrm{i}}{\nu}}+\mathrm{i}\nu-2\right) + \exp\left[-\mathrm{i}\left(t+\frac{\pi}{4}\right)\right]\left(\varepsilon\sqrt{1-\frac{2\mathrm{i}}{\nu}}+\mathrm{i}\nu+2\right)\right]. \tag{35}$$

This result shows that the asymptotic behaviour of $\langle G_{l,l}(t\to\infty)\rangle$ comes from the integral over $\mathcal{H}_1$.

For large frequencies $\nu$ we obtain from (35) the approximation

$$\langle G_{l,l}(t\to\infty)\rangle \approx -\mathrm{i}\sqrt{\frac{2}{\pi}}\frac{\nu^2}{\varepsilon^4 t^{3/2}}\cos\left(t+\frac{\pi}{4}\right). \tag{36}$$

Expression (35) is not valid for the values $\nu = 0$ and $\infty$, so for these cases we have to perform a particular analysis. Finally, note that for $\nu = \sqrt{\varepsilon^4-1}$, from (32) $g(r=1,\nu)$ diverges. Then for this frequency line the lateral $\langle G^+\rangle$ must be used in the integration (12), but this function does not have any singularity at $x=0$. Then there is no extra contribution (in the long-time regime) to (35) from the frequency line $\nu=\sqrt{\varepsilon^4-1}$.

## 5. Discussion

*Quasi-particle.* From the topological structure of the averaged Green function $\langle G_{l,l}(x)\rangle$, we can now analyse its interpretation in terms of a 'quasi-particle' because the poles of $\langle G_{l,l}(x)\rangle$ belong to the complex plane. We call a quasi-particle the excitation of the TB electron in interactions with its surroundings, i.e. the substitutional stochastic impurity located at site $l$. Then the information given by $\mathrm{Re}\,[x_k]$ and $|\mathrm{Im}\,[x_k]|^{-1}$ is related to the *energy* and the *lifetime* of the quasi-particle described before.

Now we analyse, in the space $(\nu,\varepsilon)$, the characteristics of this *energy* and *lifetime*.

- We start increasing the frequency $\nu$ but keeping $\nu<\varepsilon^2$ (until the $\delta$ points, see figure 2). Note that the energy $\mathrm{Re}\,[x_{1,2}]$ decreases while $\mathrm{Re}\,[x_{3,4}]$ increases as a function of $\nu$. When $\varepsilon^2<2$ (smaller than the band width), for increasing $\nu$, the small intensity of the noise

(impurity) does not allow the Re $[x_k]$ to go to zero *simultaneously* for all $k$, as shown in figures 2(*a*)–(*d*). On the contrary, for $\varepsilon^2 > 2$ the noise intensity is large enough to allow, for increasing $\nu$, a region in space $(\nu, \varepsilon)$ such that Re $[x_k] = 0$ for all $k$, see figures 2(*e*) and (*f*). This means that the quasi-particle has a finite lifetime but *zero* energy. From figures 3(*a*) and (*b*) the intersection region for Re $[x_k] = 0$ is characterized by $2\sqrt{\varepsilon^2 - 1} < \nu < \varepsilon^2$ (for $\varepsilon^2 > 2$) and corresponds to the line between the points $\beta$ and $\delta$ in figure 2(*e*). Note that poles $x_{3,4}$ are purely imaginary between the points $\underline{\alpha}$ and $\delta$, see figure 2(*f*). If we keep increasing the frequency but now we allow $\nu > \varepsilon^2$ (beyond the $\delta$ points in figure 2(*e*)) a remarkable result appears: the quasi-particles have *non-zero* energies; this is what we call *reentrance* of the energy [29].

- Let us analyse the case when $\nu \gg \varepsilon^2$ for all $\varepsilon$. From (23) we see that $x_{1,4}$ go to the band edges (from inside) with a long lifetime, while the poles $x_{2,3}$ approach the edges of the 'dynamical branch cut' with a short lifetime, see points $\gamma$ in figure 2.

*Dynamics.* Now we study the dynamics of the TB electron (the particle) in the space $(\nu, \varepsilon)$, which is characterized by the temporal behaviour of the averaged Green function. Using the residues on the poles $x_k$, and having performed the integration over $\mathcal{H}_1$ and $\mathcal{H}_2$, we now take into account the contributions from each term in (26) to give the total asymptotic behaviour of $\langle G_{l,l}(t)\rangle$ for $\nu \geqslant 0$ in the form

$$\langle G_{l,l}(t)\rangle \sim \mathrm{i}\sum_k M_1[x_k(\nu,\varepsilon)]\exp(-\mathrm{i}\mathrm{Re}\,[x_k]t) \times \exp(-|\mathrm{Im}\,[x_k]|t) + M_2(\nu,\varepsilon,t)(1+\exp(-\nu t))/t^{3/2} \tag{37}$$

where $M_2(\nu, \varepsilon, t)$ contains the time-dependent oscillatory part of (35). In (37) we have considered the case of having simple poles, then $M_1[x_k(\nu, \varepsilon)]$ comes from (28). This formula shows that there are two different contributions. The first one corresponds to what we have called 'dynamical localization' (given by the residue terms). The second term in (37) gives a decay of the order of $t^{-3/2}$, which is due to the presence of extended states inside the band, see figure 1. Note that the integral over the 'dynamical branch cut' on $-\mathrm{i}\nu$, see figure 4, gives a contribution exponentially smaller than the one coming from the 'static branch cut' (the band). Thus, to study the behaviour of the wave function we have to compare the magnitude of each term in (37), and analyse the characteristics of the poles in the space $(\nu, \varepsilon)$. Finally, note that the first term is valid for any time, while the last term is given in the asymptotic regime (large $t$).

The averaged dynamics of the TB electron can easily be understood in two limiting cases: the adiabatic limit $\nu \sim 0$ and the very fast fluctuation limit $\nu \gg \varepsilon^2$.

- For the special case $\nu = 0$ (points $\alpha$ in figure 2), the impurity gives rise to *only one* non-decaying localized state with energy $x_S$. Then if the particle starts in this state the quantum amplitude will not decay. When we *turn on* the dynamical impurity, $\nu \gtrsim 0$, the model has a stochastic substitutional site, i.e. in the impurity site $l$ the energy can fluctuate between the values $\pm\varepsilon$, while $\varepsilon_0 = 0$ for the rest of the lattice. Then we can say that, during a timescale of the order $\nu^{-1}$, the particle has a localized energy, say for example $x_1(\nu = 0, \varepsilon)$, but when the impurity changes its state, the particle feels the other localized energy $x_2(\nu = 0, \varepsilon)$. So, in *mean value*, when $\nu \approx 0$, the effect of a dynamical impurity is to reduce the localized energy of the TB electron. This is so because the particle has not enough time to realize the intensity of the substitutional site. Thus the *localized energy* is around Re $[x_{1,2}]$, see figures 2(*a*), (*c*) and (*e*). In this context we can see that poles $x_{1,2}$ are responsible for the peak (localized states) in the averaged DOS: compare figures 2(*e*) and 1(*b*). On the other hand, the decay time for the m.v. quantum

amplitude, at the impurity site $l$, is characterized by the inverse of the *frequency rate* of the dichotomous process $2\nu^{-1}$, see footnote 4. To understand this fact let us assume that at $t = 0$ the dichotomous process is $m(0) = 1$ so the impurity site energy is $+\varepsilon$. Then, if there is a wave packet located at site $l$, there is a certain quantum amplitude in the localized state with energy $x_1(\nu = 0, \varepsilon)$; when the dichotomous process changes to $m = -1$ the localized energy changes to $x_2(\nu = 0, \varepsilon)$, so the amplitude at the state with $x_1(\nu = 0, \varepsilon)$ decays. But the dichotomous process $m(t)$ changes once again, and so on stochastically, producing the expected exponential decay of the wave function. This *timescale* $2\nu^{-1}$ is given by $|\mathrm{Im}\,[x_k]|^{-1}$: from (18) and (20) when $\varepsilon < 1|\mathrm{Im}\,[x_k]| = \nu/2$ for all $k$; when $\varepsilon > 1$ and for $\nu \sim 0$ there are only two poles $x_{1,2}$ and they give $|\mathrm{Im}\,[x_{1,2}]| = \nu/2$, see (19).

- For the special case $\nu \gg \varepsilon^2$ (points $\gamma$ in figure 2) all the poles have $\mathrm{Re}\,[x_k] \neq 0$. On the other hand, because the lifetime $|\mathrm{Im}\,[x_{1,4}]|^{-1}$ is long it makes sense to compare the first terms of (37) against the asymptotic long-time contribution from the extended states $\mathcal{O}(t^{-3/2})$. In this region of space $(\nu, \varepsilon)$ the averaged dynamics of the TB electron starts to be different and the contributions from the 'dynamical localization' terms die down. To note this fact we have to compare in (37) the magnitude of $|M_1[x_k(\nu, \varepsilon)]|$ against $|M_2[\nu, \varepsilon, t]|$ as a function of $\nu, \varepsilon$. From expressions (29) and (36) it is possible to see that the first one is much smaller than the second. This fact means that, in this regime, the dynamics of the particle is mainly governed by the extended states; in figure 1($e$) we see that, when $\nu \gg \varepsilon^2$, the averaged DOS for the localized states goes to zero very fast outside the band edges. Note that for $\nu \gg \varepsilon^2$ the poles fulfil $|\mathrm{Re}\,[x_{1,4}]| < 1$ and $|\mathrm{Im}\,[x_{1,4}]| \sim 0$, then one could expect a resonant-like peak inside the band in the $\mathcal{D}_{\mathrm{DOS}}$ (even in one dimension). But this is not seen from figures 1($c$) and ($d$) where it is possible to realize that both maxima approach the band edges from outside. In the limit $\nu = \infty$, the fast fluctuation of the impurity completely erases the different energy at site $l$ (averaging $\pm\varepsilon$ to zero) so we recover the TB homogenous case. From a simple analysis of (23) poles $x_{1,4} \to \pm 1$ for infinite frequency $\nu$. The other poles $x_{2,3}$ go to the 'dynamical branch cut' at $-\mathrm{i}\infty$, so in this limit they do not contribute to the temporal behaviour of the wave function.

*Final conclusions.* To end this section we conclude that the singularities of the averaged Green function govern the dynamics of the TB electron given by $\langle G_{l,l}(t)\rangle$. This analysis is inspired by Messiah's book [30] when he studied the behaviour of an open quantum system in terms of the Green function and its complex self-energies. In our case the quantity $|\mathrm{Im}\,[x_k]|^{-1}$ gives a timescale within which the observer can interpret the dynamical localization phenomena from the residues contribution of (37), i.e. for times $t$ fulfilling $|\mathrm{Im}\,[x_k]|\ t \ll 1$ the particle is localized, and for times $|\mathrm{Im}\,[x_k]|\ t \gg 1$ the TB electron behaves as an extended particle. Therefore the region where there is dynamical localization corresponds to a quasi-particle with finite energy. The lifetime of the quasi-particles (the delocalization time of the TB electron) indicates irreversible processes occurring in the open system, in our case being represented by a stochastic perturbation in the Hamiltonian.

We can also conclude that the singularities and the dynamical behaviour of the wave function are related to the typical energies of the system. For example, we have emphasized that the reentrance phenomena only appears if the intensity of the impurity $\varepsilon^2$ is larger that the band width. On the other hand, the dynamics of the wave function is governed by the extended states only when $\varepsilon^2/\hbar\nu \ll 2v_0$ (in dimensional units). So a non-trivial relation between $\varepsilon$ and $\nu$ gives the strength of the stochastic perturbation at the impurity site $l$.

We end this paper by noting that, if we think that the stochastic character of the Hamiltonian represents internal fluctuations produced by a thermal bath at temperature $T$ (that can be related

to the frequency $\nu$), the averaged DOS helps to calculate *effective* equilibrium thermodynamics quantities; for example, the specific heat, etc. The $n$-dimensional TB chain can in principle also be worked out, but we are confident that the basic consequences of a stochastic impurity can just be studied from a 1D model. The case when the dichotomous process $m(t)$ is not symmetric (asymptotically in time the mean value does not go to zero) can also be studied in a similar way; in this case we expect that in the very fast frequency $\nu$ limit the fluctuation of the impurity does not erase the substitutional energy site. Thus in this limiting case we will not arrive at the behaviour of a homogeneous TB model. The interesting case when there are many fluctuating impurities can be worked out by introducing a sort of effective medium approximation [31] for dynamical disorder [15]; this work is in progress.

## Acknowledgments

AKCh thanks a fellowship from *Fundación Antorchas*. MOC thanks CONICET for grant no 4948/96. We thank Karen Hallberg for the critical English revision of the manuscript.

## Appendix. White-noise case

In this appendix we analyse the particular case of a Gaussian white-noise impurity. Therefore Novikov's theorem [12] can be used to calculate $\langle G(t)\rangle$ from the TB Hamiltonian $H = H_0+\omega(t)V_l$, when $\omega(t)$ is Gaussian white noise with intensity $D$ characterized by the correlation $\langle\omega(t)\omega(t')\rangle = D\delta(t-t')$. So we obtain for the diagonal elements of the averaged Green function (in adimensional units $2v_0 = 1, \hbar = 1$)

$$\langle G(x)_{l,l}\rangle_{wn} = \frac{1}{\sqrt{x^2-1}+\mathrm{i}D/2}. \tag{A.1}$$

This result is in agreement with the calculation of the dichotomous process in the limit $\varepsilon^2 \to \infty$, $\nu \to \infty$ with $\varepsilon^2/\nu \to D/2$. In this limit the effective energy $\tilde{\varepsilon}_d$ goes to $\tilde{\varepsilon}_{wn} = -\mathrm{i}D/2\hbar$, see (9).

The averaged Green function looks similar to the static impurity case, but with a pure imaginary energy $\tilde{\varepsilon}_{wn}$ at site $l$. From this fact the averaged DOS $\pi\mathcal{D}_{\mathrm{DOS}}(x,l) = -\mathrm{Im}\,\langle G^+(x)_{l,l}\rangle_{wn}$ shows that there are extended states inside the band and there are also localized states outside the band, but this density (outside the band) is smaller than for the case of a dichotomous noise. In figure 5 we have compared the Gaussian against the dichotomous case for the same intensity: $D/2 = \varepsilon^2/\nu = 3/10$. Note that for the Gaussian case the averaged DOS at the band edges has a finite value $\pi\mathcal{D}_{\mathrm{DOS}}(\pm 1, l) = 2/D$, while for the dichotomous case it diverges at the band edges when $\nu \to \infty$ (going in average to the TB homogeneous DOS). It is also possible to see that, for large or small values of $D$, the $\mathcal{D}_{\mathrm{DOS}}$ for the Gaussian case looks quite similar. Of course, for any value of $D$ there is no 'peak' in the averaged DOS (as in the case of a dichotomous impurity, see figure 1($a$)–($c$)) due to the purely imaginary nature of the effective energy $\tilde{\varepsilon}_{wn}$. Trivially in the $D \to 0$ limit we reobtain the TB homogeneous DOS, as expected.

In order to obtain the asymptotic temporal behaviour of the averaged Green function we now look for the singularities of (A.1), showing a branch cut on the real axis when $|x| \leqslant 1$ and simple poles. For $D < 2$ the poles are in the real positions $x_{\pm}^{wn} = \pm\sqrt{1-\frac{D^2}{4}}$ (inside the band), but we can see that they are poles only for the lateral Green function $\langle G^-_{l,l}\rangle_{wn}$. For $D > 2$ there is only one purely imaginary pole $x^{wn} = -\mathrm{i}\sqrt{\frac{D^2}{4}-1}$ and it falls under the band. Thus we reobtain the results of section 4.1 when taking the Gaussian limit from the poles of the dichotomous process (24) and (25).

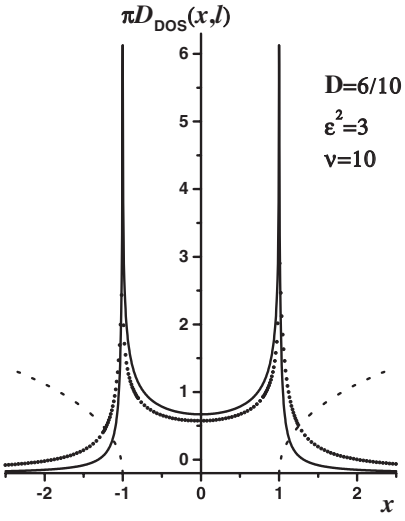


**Figure 5.** DOS per site $\pi\mathcal{D}_{\mathrm{DOS}}(x,l)$ versus $x$. We have compared the Gaussian white-noise case with $D/2 = 3/10$ (full curve) against the dichotomous case for $\varepsilon^2 = 3$ and $\nu = 10$ (circled curve). There is no peak in the Gaussian case for any value of $D$. At the band edges the averaged DOS has a finite value. The dotted curves correspond to $\lambda^{-1}(x)$ for both cases.

In order to understand the averaged dynamics of the TB electron, we now calculate the asymptotic temporal behaviour of $\langle G(t)_{l,l}\rangle_{wn}$. As before we have to consider the residues on the poles inside the contour of integration and the contribution from the branch cut is calculated, asymptotically, as in section 4.2.

For $D < 2$ the poles are not inside the contour of integration and the asymptotic behaviour comes from the branch cut, so

$$\langle G(t\to\infty)_{l,l}\rangle_{wn} \sim -\frac{4\mathrm{i}}{D^2}\sqrt{\frac{2}{\pi t^3}}\cos\left(t+\frac{\pi}{4}\right).$$

The $t^{-3/2}$ tendency is similar to the case when the TB electron is in the presence of a static impurity, but now there is no localization effect due to the purely imaginary nature of the energy $\tilde{\varepsilon}_{wn}$, see (A.1).

For $D > 2$ there is only one pole inside the contour of integration and the behaviour is

$$\langle G(t\to\infty)_{l,l}\rangle_{wn} \sim \frac{\mathrm{i}D}{2\sqrt{\frac{D^2}{4}-1}}\exp\left[-t\sqrt{\frac{D^2}{4}-1}\right] - \frac{4\mathrm{i}}{D^2}\sqrt{\frac{2}{\pi t^3}}\cos\left(t+\frac{\pi}{4}\right). \tag{A.2}$$

Although there is a pole the averaged Green function does not show any dynamical localization. Note that the first term of (A.2) can also be interpreted in terms of a quasi-particle with zero energy and finite lifetime of the order $1/\sqrt{\frac{D^2}{4}-1}$. We conclude that for the Gaussian dynamical impurity (even with an intensity higher that the band width) the $\langle G(t)\rangle_{wn}$ is not affected by the localized states showed in the averaged DOS, figure 5. The non-correlated fluctuations of the Gaussian white-noise erase, on average, the presence of the dynamical impurity, giving rise to a TB dynamics mainly governed by its extended states.

## References

[1] Madhukar A and Post W 1977 *Phys. Rev. Lett.* **39** 1424
[2] Boden N, Bushby R, Clemens J, Donovan K, Movaghar B and Kreouzis T 1998 *Phys. Rev.* B **58** 3063
[3] Sheng P 1990 *Scattering and Localization of Classical Waves in Random Media* (Singapore: World Scientific)
[4] Jayannavar A M and Kumar N 1982 *Phys. Rev. Lett.* **48** 553
[5] Jayannavar A M 1993 *Phys. Rev.* E **48** 837

[6] Bernier D and Maschke K 1991 *J. Phys.: Condens. Matter* **3** 2881
[7] Bouchaud J P 1990 *Europhys. Lett.* **11** 505
Bouchaud J P, Touati D and Sornette D 1992 *Phys. Rev. Lett.* **68** 1787
[8] Hunt J G, Bloor D and Movaghar B 1983 *J. Phys. C: Solid State Phys.* **16** L623–8
[9] Gurvitz S A 2000 *Phys. Rev. Lett.* **85** 812
[10] Anderson P W 1954 *J. Phys. Soc. Japan* **9** 316
[11] Kubo R 1954 *J. Phys. Soc. Japan* **9** 935
[12] van Kampen N G 1992 *Stochastic Proceses in Physics and Chemistry* 2nd edn (Amsterdam: North-Holland)
[13] Bourret R S, Frisch U and Pouquet A 1973 *Physica* **65** 303–20
[14] Shapiro V E and Loginov V M 1978 *Physica* A **91** 563
[15] Budde C E and Cáceres M O 1988 *Phys. Rev. Lett.* **60** 2712
[16] Inaba Y 1981 *J. Phys. Soc. Japan* **50** 2473
[17] Kraus V and Reineker P 1991 *Phys. Rev.* A **43** 4182
[18] Goycuk I A, Petrov E G and May V 1998 *Phys. Lett.* A **238** 59
[19] Pury P A and Cannas S A 1991 *J. Phys. A: Math. Gen.* **24** L1405–14
[20] Economou E N 1983 *Green Functions in Quantum Physics* 2nd edn (Berlin: Springer)
[21] Gonis A 1992 *Green Functions for Ordered and Disordered Systems* (New York: North-Holland)
[22] Crisanti A, Paladin G and Vulpiani A 1993 *Products of Random Matrices (Springer Series in Solid State Sciencies vol 104)* (Berlin: Springer)
[23] Anderson P W 1958 *Phys. Rev.* **109** 1492
[24] Loyd P L 1969 *J. Phys. C: Solid State Phys.* **2** 1717
[25] Ishii K 1973 *Prog. Theor. Phys. Suppl.* **53** 77
[26] Budini A A, Chattah A K and Cáceres M O 1999 *J. Phys. A: Math. Gen.* **32** 631
[27] Doetsch G 1971 *Guide to Applications of the Laplace and B-Transforms* (London: van Nostrand-Reinhold)
[28] Haken H 1983 *Quantum Field Theory of Solids: An Introduction* (Amsterdam: North-Holland)
[29] Cáceres M O and Chattah A K 2000 *Phys. Lett.* A **276** 272
[30] Messiah A 1969 *Quantum Mechanics* (Amsterdam: North-Holland) chapter 21, section 13
[31] Caceres M O, Matsuda H, Odagaki T, Prato D P and Lamberti W 1997 *Phys. Rev.* B **56** 5897